Short-chain chlorinated paraffins (SCCPs) disrupt hepatic fatty acid metabolism in liver of male rat via interacting with peroxisome proliferator-activated receptor α (PPARα)

Yufeng Gong[a], Haijun Zhang[a,*], Ningbo Geng[a], Xiaoqian Ren[a,b], John P. Giesy[c,d], Yun Luo[a,b], Liguo Xing[e], Ping Wu[a], Zhengkun Yu[a], Jiping Chen[a]

[a] CAS Key Laboratory of Separation Sciences for Analytical Chemistry, Dalian Institute of Chemical Physics, Chinese Academy of Sciences, Dalian, 116023, Liaoning, China
[b] University of Chinese Academy of Sciences, Beijing, 100049, China
[c] Department of Veterinary Biomedical Sciences and Toxicology Centre, University of Saskatchewan, Saskatoon SK, S7N 5B4, Saskatchewan, Canada
[d] Department of Environmental Science, Baylor University, Waco TX, 76706, Texas, United States
[e] Safety Evaluation Center of Shenyang Research Institute of Chemical Industry Ltd, Shenyang, 110021, Liaoning, China

A B S T R A C T

Short-chain chlorinated paraffins (SCCPs) are frequently detected in environmental matrices and human tissues. It was hypothesized that SCCPs might interact with the peroxisome proliferator-activated receptor α (PPARα). In the present study, an *in vitro,* dual-luciferase reporter gene assay and *in silico* molecular docking analysis were employed together to study the interactions between SCCPs congeners and PPARα. Expressions of genes downstream in pathways activated by PPARα in liver of rats exposed to 1, 10, or 100 mg/kg bm/d of C_{10-13}-CPs (56.5% Cl) for 28 days were examined to confirm activation potencies of SCCPs toward PPARα signaling. Effects of exposure to C_{10-13}-CPs (56.5% Cl) on fatty acid metabolism in rat liver were also explored via a pseudo-targeted metabolomics strategy. Our results showed that C_{10-13}-CPs (56.5% Cl) caused a dose-dependent greater expression of luciferase activity of rat PPARα. Molecular docking modeling revealed that SCCPs had a strong capacity to bind with PPARα only through hydrophobic interactions and the binding affinity was dependent on the degree of chlorination in SCCPs congeners. In livers of male rats, exposure to 100 mg/kg bm/d of C_{10-13}-CPs (56.5% Cl) resulted in up-regulated expressions of 11 genes that are downstream in the PPARα-activated pathway and regulate catabolism of fatty acid. Consistently, accelerated fatty acid oxidation was observed mainly characterized by lesser concentrations of Σfatty acids in livers of rats. Overall, these results demonstrated, for the first time, that SCCPs could activate rat PPARα signaling and thereby disrupt metabolism of fatty acid in livers of male rats.

1. Introduction

Metabolic diseases could be associated with exposure to pollutants (Feige et al., 2010; Fletcher et al., 2013; Harley et al., 2013; Lejonklou et al., 2017; Matilla-Santander et al., 2017; Uemura et al., 2009). Among various environmental pollutants, due to their occurrences in blood of humans, short-chain chlorinated paraffins (SCCPs) are of particular concern (Li et al., 2017). SCCPs are polychlorinated derivatives of *n*-alkanes with lengths of carbon chains of 10–13 and chlorine contents of 30%–70% (Fiedler et al., 2010). As a constituent of chlorinated paraffins (CPs), SCCPs are used for various industrial applications, such as flame retardants, plasticizers, metal-working fluids, lubricant additives, paints, sealants, and leather fat liquors. Worldwide production of SCCPs exceeded 165,000 tons in 2016, and their cumulative production volume has been estimated to be greater than 2 million tons (Glüge et al., 2016). Due to their environmental persistence, potentials for bioaccumulation and long-range atmospheric transport, in 2017, the Stockholm Convention listed SCCPs as a new group of persistent organic pollutants (POPs) (Li et al., 2016; Ma et al., 2014; United Nations Environment Program , 2017; Zeng et al., 2017).

SCCPs exhibited hepatotoxicity, developmental toxicity, endocrine disrupting activity and carcinogenicity (Ali et al., 2010; Burýšková

---

et al., 2006; Gong et al., 2018; Liu et al., 2016; Warnasuriya et al., 2010; Zhang et al., 2016). Recently, impairments of metabolism, especially for lipid metabolism, were observed in human liver cells and zebrafish larvae after SCCPs exposure (Ren et al., 2018; Wang et al., 2018). However, the underlying mechanisms of adverse effects of SCCPs remain elusive.

SCCPs have an aliphatic structure, which is similar to those of natural ligands (fatty acids) of peroxisome proliferator-activated receptor α (PPARα). PPARα plays a major role in metabolic regulation, especially for metabolism of fatty acids (Kersten et al., 2014). PPARα is a ligand-dependent transcription factor, which is expressed in high-metabolic rate tissues, such as liver and brown adipose tissue (Poulsen et al., 2012). Once activated, PPARα regulates expressions of genes via binding to a specific peroxisome proliferator response element (PPRE) in or around target genes. To date, PPARα has been identified as a key factor in pathogenesis of numerous human diseases (Kersten et al., 2000). Toxicity caused by exposure to SCCPs matched well with that by PPARα agonist, such as non-genotoxic carcinogens and peroxisome proliferation (Bucher et al., 1987; Nilsen et al., 1981; Serrone et al., 1987). Given the above information, it was hypothesized that SCCPs might interact with the PPARα signaling pathway to bring about detrimental metabolic effects.

Thus, to address this issue, the ability of SCCPs to activate PPARα was first assessed by use of a transactivation assay with luciferase as a reporter gene under control of rat PPARα in the present study. Then, the influence of SCCPs on PPARα signaling was further determined by examining expressions of PPARα downstream genes *in vivo* in liver of male, Sprague Dawley (SD) rats exposed orally to SCCP. Also, molecular docking simulations were conducted to explore modes of binding of SCCP congeners to the ligand-binding pocket (LBP) of PPARα. Finally, effects of SCCPs on metabolism of fatty acids in rat liver were investigated using a pseudo-targeted metabolomics strategy. Our results provided insight into the mode of action of SCCPs in the perturbation of fatty acid metabolism.

2. Materials and methods

2.1. Chemicals and cells

A SCCPs mixture, C_{10-13}-CPs (C_{10}-CPs: C_{11}-CPs: C_{12}-CPs: C_{13}-CPs mass ratio = 1: 1: 1: 1; Cl content: 56.5%), was synthesized by the chlorination of *n*-alkanes as described elsewhere (Tomy et al., 2000). Here, the C_{10-13}-CPs mixture (Cl content: 56.5%) was employed as an example of a realistic environmental exposure scenario. Human embryonic kidney 293 T cells were purchased from China Infrastructure of Cell Line Resources (Shanghai, China). Cells were cultured in Dulbecco's Modified Eagle's Medium (DMEM; Gibco-BRL, USA) supplemented with 10% fetal bovine serum and 1% penicillin-streptomycin (Beyotime, China) under a humidified atmosphere of 5% CO_2 and 95% air at 37 °C. Cells at the exponential growth phase were used for the experiment.

2.2. Transfection and luciferase assay

Kidney 293 T cells were used to determine transactivation of rat PPARα by SCCPs because they offer several advantages such as easy growth and transient transfection, and they are suitable for the present study because those cells express little or no endogenous PPARα (Figure S1 of Supplementary material). The rat-derived PPRE-firefly luciferase reporter plasmids (pGL4.26-rPPRE-Luc) and expression plasmids for rat PPARα ligand binding domain (p3xFlag-rPPARα/hPPARα) were purchased from TranSheep (Shanghai, China). 293 T cells were seeded in 24-well plates at 1×10^4/well and transiently co-transfected with 90 ng of PPRE-firefly luciferase reporter plasmid and 5 ng of expression plasmid, either empty or coding for rat PPARα using Lipofectamine 2000 reagent (Life Technologies) for 48 h. After replacing the culture

medium, cells were treated with test chemicals for 24 h to evaluate PPARα agonistic activity. 0.5% DMSO served as the solvent and no precipitation was observed for all test chemicals. Cells were washed once in cold, phosphate-buffered saline (PBS; pH 7.4) and lysed with reporter lysis reagent for 15 min. Luciferase activities were assayed using the luciferase reporter assay kit (Promega, USA). Luciferase activity in the negative control group was assigned a value of 1.0.

2.3. In vivo rat exposure experiment

Animal usage for the study and euthanasia procedure were reviewed and approved by the animal ethics committee of Safety Evaluation Center, Shenyang Research Institute of Chemical Industry (Approval number R14FO10010). Ethical regulations were followed according to the national guidelines for the protection and care of experimental animals. Thirty-two male SD rats (approximately 5 weeks old; 339–407 g body mass (bm)) were housed in controlled conditions (25 ± 3 °C, 40%–50% humidity, one animal per cage) under a 12 h light/dark cycle. Food and water were provided *ad libitum*. After a 5-d acclimatization, rats were randomized into 4 groups (8 rats per group) and treated with corn oil (vehicle; 5 mL/kg bm/d) or various dosages (1, 10, or 100 mg/kg bm/d) of C_{10-13}-CPs (56.5% Cl) by gavage for 28 d. Exposure doses were determined according to the no observed adverse effect level (NOAEL, 10 mg/kg bm/d) for rats (United Nations Environment Program, 2017). By the end of the exposure, rats were anesthetized with diethyl ether. Liver tissues were removed during necropsy, snap-frozen (liquid nitrogen), and stored at −80 °C before gene expression analysis and metabolite analysis.

2.4. Isolation of mRNA and quantitative real-time polymerase chain reaction (qPCR) analysis

Total RNA was isolated using the Takara RNAiso Plus reagent (Takara, Tokyo, Japan). qPCR was performed on the Light Cycler 480 PCR System (Roche Diagnostics, Mannheim, Germany) using a FastStart Universal SYBR Green Master kit (Roche Applied Science, Mannheim, Germany). Amounts of mRNA for each gene were quantified and then normalized to the geometric mean of internal references (*Actb* and *Gapdh*) by use of the $2^{-\triangle\triangle Ct}$ method (Livak and Schmittgen, 2001). Primers used are listed in Supplementary Table S1.

2.5. Molecular docking

LeDock (http://lephar.com) was used to simulate binding of SCCPs to PPARα protein. Initial conformations of 46 SCCP congeners were downloaded from the SciFinder database (https://scifinder.cas.org) (Supplementary Table S2). Three crystal structures of human PPARα in complex with different agonists (PDB No. 4BCR, 2P54, and 3VI8) were used for ensemble docking. Crystalized water and the co-crystalized ligand were removed, and hydrogen atoms were added to the protein according to the protonation states of the chemical groups at pH 7.0. The binding cavity was generated and centered on the endogenous ligand-bound site of PPARα ligand-binding domain with the box size extending in x, y, and z directions with a radius of 5 Å. All molecules in docking calculations have geometry optimizations. Binding energies between the SCCP molecules and PPARα by LeDock were also calculated for binding affinity comparison.

2.6. Identification and quantifications of metabolites

Rat liver samples were first homogenized and then ultrasonicated in an ice-water bath. Samples were subsequently freeze-dried and extracted with a mixture of methanol/water (4:1, v:v). Prior to extraction, three kinds of internal standards were spiked into the sample for quality control of sample preparation and instrumental analysis. Details on preparation of samples are given in Supplementary material. A pseudo-

targeted metabolomics analysis was conducted to detect fatty acids, acylcarnitines, and free L-carnitine (Chen et al., 2013). In brief, an untargeted analysis was first conducted using an Agilent 1290 Infinity ultra-high performance liquid chromatography system coupled online to an Agilent 6540 UHD Q-TOF MS (Agilent, Santa Clara, CA) system (UHPLC/Q-TOF MS) to acquire ion pair information, including precursor ions, product ions, and collision energies. Information on ion pairs was further combined and used for the following targeted analysis. In the targeted analysis program, a Waters Acquity, ultra-high performance liquid chromatography coupled online to an ABI Q-Trap 5500 (ABSCIEX, USA) system (UHPLC/Q-Trap MS) was operated in multiple reaction monitoring mode (MRM) to detect all metabolites in samples by use of previously described methods (Ren et al., 2018; Wang et al., 2016). Raw metabolomics data were processed by MultiQuant software (3.0.1, AB SCIEX). After peak alignment and missing value interpolation, the peak areas of each metabolite were normalized to corresponding internal standards.

2.7. Statistical analyses

Metabolic effect level index (MELI) values were calculated to assess overall alteration of fatty acid metabolism after exposure to SCCPs (Details in Supplementary material) (Riedl et al., 2015). To compare responses and determine significant differences, part of the data is presented as the mean $\pm$ standard error (SE). Metabolomics data were log-transformed and auto-scaled by using MetaboAnalyst 4.0. Following testing for the normality assumption and variance homogeneity, one-way analysis of variance (ANOVA) followed by Student's t-test were employed to evaluate the significance of the mean differences. Differences were considered significant at $0.01 < P < 0.05$ and highly significant when $P < 0.01$. Pearson correlation analysis and related P-values were employed to describe the correlations.

3. Results

3.1. Activation of rat PPARα by SCCPs

In the present study, a transactivation assay with firefly luciferase as a reporter gene under control of rat PPARα was employed to study potentials of SCCPs to activate rat PPARα signaling. Before conducting luciferase assays, a 3-[4,5-dimethylthiazolyl-2]-2,5-diphenyltetrazoliumbromide (MTT) assay was performed to investigate the effect of C_{10-13}-CPs (56.5% Cl) on viability of cells. No significant changes in cell viability were observed in 293 T cells exposed to C_{10-13}-CPs (56.5% Cl) at 0.0036–18.075 mg/l, i.e., 0.01–50 μM, for 24 h (Supplementary Figure S2). Concentrations of 0.036, 0.362, 0.723, and 1.808 mg/l, i.e., 0.1, 1, 2, and 5 μM, were then used in the luciferase reporter assay. A potent PPARα activator, pirinixic acid (WY-14643) (CAS No. 50892-23-4), was used as a positive control. In vitro PPARα reporter gene assay displayed a significant response to 1 μM of pirinixic acid (Supplementary Figure S3). No significant responses were observed in non-PPARα-transfected cells exposed to pirinixic acid, which indicated validity of the reporter gene assay.

Similar to treatment with pirinixic acid, exposure of cells with C_{10-13}-CPs (56.5% Cl), caused a dose-dependent greater expression of luciferase activity of rat PPARα relative to the control group, and the maximal induction was 2.04 ± 0.04-fold ($P = 4.02E-5$) (Fig. 1). Compared with the rat PPARα-transfected groups, luciferase activities in non-rat PPARα transfected groups were significantly less, suggesting that induction of luciferase was PPARα-specific. Together, these results demonstrated transactivation potencies of SCCPs toward rat PPARα.

3.2. Expression of PPARα downstream genes in livers of rats

Expression of classical downstream genes of PPARα was quantified in liver of male rats after exposure to C_{10-13}-CPs (56.5% Cl) for 28
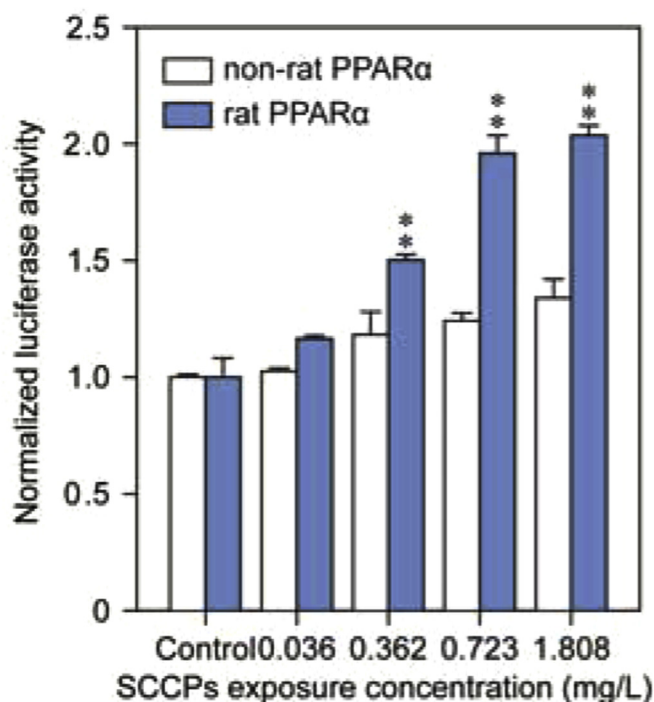
Fig. 1. Modulation of transcription of rat PPARα by C_{10-13}-CPs (56.5% Cl), as determined by an *in vitro* luciferase reporter gene assay. Asterisks indicate statistically significant differences from the control group (*$P < 0.05$; **$P < 0.01$). $N = 3$.

days. These genes included *Pex11a*, *Decr2*, *Ech1*, *Ehhadh*, *Acaa1*, *Acadl*, *Acadvl*, *Decr1*, *Eci1*, *Hadha*, and *Cyp4a1*. All of these genes are considered to be at least partly regulated by PPARα (Kersten et al., 2014; Mandard et al., 2004; Rakhshandehroo et al., 2010). See Supplementary material for more information about these genes.

Exposure to SCCPs altered expression of genes modulated by PPARα in rat liver. Exposure to 100 mg C_{10-13}-CPs/kg bm/d (56.5% Cl) significantly up-regulated expression of mRNA of all 11 test genes (Fig. 2). This data was consistent with results of the luciferase assay and further supported the activation of rat PPARα signaling by *in vivo* exposure to SCCPs. However, no significant up-regulations of these genes were observed in liver of rat exposed to 1 or 10 mg/kg bm/d, relative to the control group. In addition, exposure to 10 mg C_{10-13}-CPs/kg bm/d (56.5% Cl) resulted in significantly less expression of mRNA for *Acaa1* (0.48 ± 0.13-fold; $P = 0.02$) in rat liver.

3.3. Simulations of modes of bindings

To better understand the structural basis for observed interactions between SCCPs and signaling modulated by PPARα, molecular docking simulations were conducted, by use of LeDock software (Zhao and Caflisch, 2014). Binding energies were calculated to compare strength of binding to the PPARα receptor among ligands. To account for flexibility of the protein, SCCPs were docked into each of the three distinct PPARα structures (4BCR, 2P54, and 3VI8), and the greatest binding affinity was chosen. A total of 46 SCCP structures with varying carbon chain lengths (from C_{10} to C_{13}) and chlorine contents (from 16.22% to 72.92%) were analyzed. Pirinixic acid was used as a positive reference. Binding of perfluorooctanoic acid (PFOA), perfluorooctanesulfonic acid (PFOS), and 4 natural saturated fatty acids with carbon chain lengths of 10–13 (*n*-decane acid, *n*-undecanoic acid, *n*-dodecanoic acid, and *n*-tridecanoic acid) were also determined.

Based on results of molecular docking, predicted binding affinities of pirinixic acid, PFOA, and PFOS to PPARα were -8.49, -6.30, and -7.37 kcal/mol, respectively. Binding affinities of the four saturated
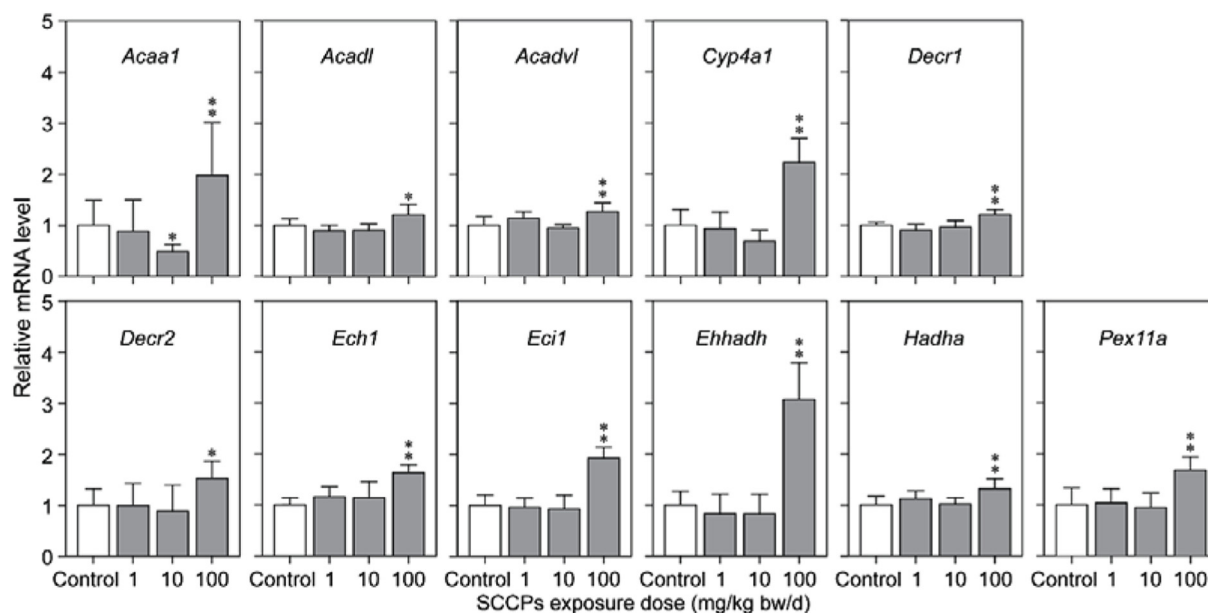
Fig. 2. Quantitative analysis of expressions of classical genes modulated by PPARα in male rats exposed orally to 1, 10 or 100 mg C_{10-13}-CPs/kg bm/d (Cl content: 56.5%) for 28 d. Asterisks indicate statistically significant differences from the control group (*$P < 0.05$; **$P < 0.01$). $N = 8$. *Acaa1*: acetyl-CoA acyltransferase 1A; *Acadl*: acyl-CoA dehydrogenase, long chain; *Acadvl*: acyl-CoA dehydrogenase, very long chain; *Cyp4a1*: cytochrome P450, family 4, subfamily a, polypeptide 1; *Decr1*: 2,4-dienoyl-CoA reductase 1; *Decr2*: peroxisomal 2,4-dienoyl-CoA reductase; *Ech1*: enoyl-CoA hydratase 1, peroxisomal; *Eci1*: enoyl-CoA delta isomerase 1; *Ehhadh*: enoyl-CoA hydratase/3-hydroxyacyl CoA dehydrogenase; *Hadha*: hydroxyacyl-CoA dehydrogenase trifunctional multienzyme complex subunit alpha; *Pex11a*: peroxisomal biogenesis factor 11 alpha.

fatty acids to PPARα ranged from −5.24 to −6.29 kcal/mol. In contrast, SCCPs exhibited affinities of binding to PPARα ranging from −5.30 to −9.16 kcal/mol for C_{10}-CPs, from −5.33 to −9.97 kcal/mol for C_{11}-CPs, from −5.87 to −9.63 kcal/mol for C_{12}-CPs, and from −5.90 to −10.1 kcal/mol for C_{13}-CPs, respectively (Supplementary Table S2). Binding affinities of lesser-chlorinated SCCPs and more-chlorinated SCCPs are equivalent to and greater than those of positive and comparison references, respectively. These results indicated that SCCPs have a greater capacity to bind with PPARα. Predicted binding affinities were also linearly correlated with chlorine contents of SCCPs (Fig. 3A), with Pearson, product-moment correlation coefficients (R) of −0.972, −0.971, −0.980, and −0.973 for C_{10}-CPs, C_{11}-CPs, C_{12}-CPs, and C_{13}-CPs, respectively. These results suggested that more-chlorinated SCCPs were more tightly bound to PPARα. In addition, SCCPs preferentially bound to the hydrophobic cleft of the LBP of PPARα via hydrophobic interactions (Fig. 3B) with amino acid residues Ile241, Ile272, Ile339, Val332, Met330, Met355, Leu321, Cys275, and Cys276. There were no hydrogen-bond interactions between SCCPs and the ligand-dependent activation function (AF-2) region.

3.4. SCCPs disrupted metabolism of fatty acids in rat liver

To further illustrate roles of PPARα-mediated responses in mediation of adverse effects, specific effects of SCCPs on metabolism of fatty acids were investigated. Results of pseudo-targeted metabolomics were used to identify and quantify 25 fatty acids and 12 acylcarnitines in rat liver. Free L-carnitine was also detected and quantified. MELI values for all quantified metabolites involved in metabolism of fatty acids ($MELI_{FA}$) were calculated to compare the overall metabolism of fatty acids in response to exposure to SCCPs. For male rats, oral exposure to C_{10-13}-CPs (56.5% Cl) resulted in significantly greater $MELI_{FA}$ values in a dose-dependent manner (Supplementary Figure S4).

Oral exposure to C_{10-13}-CPs (56.5% Cl) resulted in significantly lesser total concentrations of quantified fatty acids in livers of rats (Fig. 4). Compared with the control group, mean concentrations of total quantified fatty acids were significantly less by 27.4% ($P = 4.91E-5$),

42.6% ($P = 1.21E-6$), and 46.2% ($P = 1.26E-7$) in 1, 10, or 100 mg/kg bm/d groups, respectively. Long-chain (C_{13-21}) fatty acids (LC-FA) and very long-chain ($C_{\geq 22}$) fatty acids (VLC-FA) were most abundant in livers of rats. Measured concentrations of both were significantly lesser in all groups exposed to SCCPs. Due to the abnormity of chromatographic peaks or lesser abundances, medium-chain (C_{6-12}) fatty acids (MC-FA) and short-chain ($C_{\leq 5}$) fatty acids were not quantified. For acylcarnitines, the measured concentrations of long-chain acylcarnitines (LC-AC) were significantly greater in livers of rats exposed to all doses of SCCPs, whereas no significant differences in concentrations of short-chain acylcarnitine (SC-AC) and medium-chain acylcarnitine (MC-AC) were observed between the control group and those exposed to SCCPs. Concentrations of L-carnitine in livers of rats exposed to SCCPs were also not significantly different from that of the control group.

4. Discussion

Ubiquitous occurrences of SCCPs in environmental and human samples suggest that SCCPs should be regarded as a special class of pollutant whose cellular targets and potential effects require a much better understanding. However, although there are lots of efforts have been taken, the toxicity target of SCCPs remains largely unknown (Cooley et al., 2001; Kato and Kenne, 1996; Liu et al., 2016; Warnasuriya et al., 2010). By combining multiple bioassays and *in silico* modeling, our study is the first to reveal that PPARα is one of the potential toxicity targets of SCCPs. The insight into the toxicity target of SCCPs is valuable to understand their toxicological mechanisms and helps to ensure their safe uses in the environment.

4.1. Exposure to SCCPs activated rat PPARα signaling

The luciferase assay showed that micromole concentrations of SCCPs could activate rat PPARα (Fig. 1). Meanwhile, in rat liver, agonistic activity of SCCPs to PPARα pathways were further validated by observations of up-regulated expressions of 11 classical genes after the
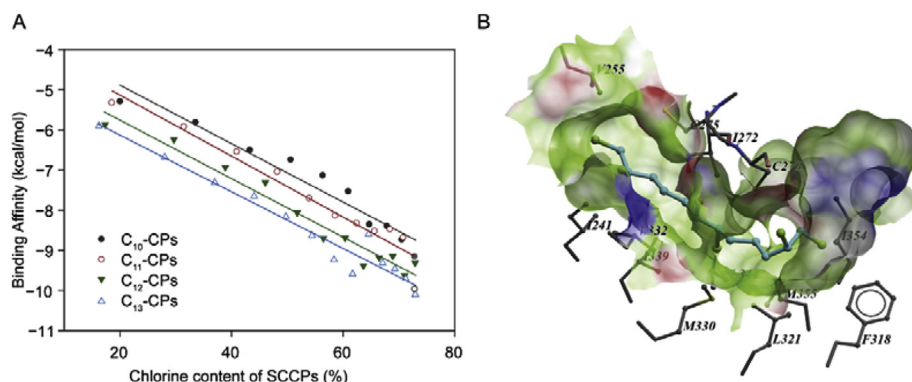
Fig. 3. Computational docking study. (A) Binding affinities (kcal/mol) between various SCCPs and PPARα. (B) Predicted binding mode of $C_{12}Cl_6$-CPs in the LBP of PPARα (PDB code 2P54). The binding pocket is illustrated by the molecular surface, with carbon in green, oxygen in red, and nitrogen in blue. Protein residues within 5 Å of the ligand are shown in stick format, with carbon in gray, oxygen in red, and nitrogen in blue. $C_{12}Cl_6$-CPs is shown with carbon in cyan. (For interpretation of the references to colour in this figure legend, the reader is referred to the Web version of this article.)

and hepatocellular carcinoma (Bucher et al., 1987; Nilsen et al., 1981; Serrone et al., 1987), were most prominently attributed to transactivation of PPARα.

4.2. SCCPs interact with PPARα LBP only through hydrophobic contacts

To better understand the structural basis for the observed effects of SCCPs on PPARα signaling, molecular docking analyses were conducted. Because of high identity (92%) in amino acid sequences between rat and human PPARα and lack of rat PPARα structure in PDB database, the structure of the human PPARα derived from X-ray diffraction data was used to study the interaction between SCCPs and PPARα. Recently, a new LBP (2nd LBP) in the crystal structure of human PPARα was identified by Bernardes et al. (2013). However, long-chain perfluoroalkyl substances (PFASs) didn't fit into the 2nd LBP of human PPARα (Ishibashi et al., 2019). Previous studies indicated that molecular docking analysis solely dealing with the classical LBP of PPARα could also provide good prediction accuracy (Li et al., 2018). Thus, considering the structure similarity between SCCPs and long-chain PFASs, we focused on the classical LBP of human PPARα in the present study.

Based on results of *in silico* simulation, SCCP congeners exhibited significant binding affinity to PPARα (Fig. 3A). However, SCCPs were bound to the PPARα LBP only via hydrophobic interactions (Fig. 3B). The PPARα LBP contains an AF-2 region (Brélivet et al., 2012). Most PPARα agonists, such as PFOA, form hydrogen bonds with residues on the AF-2 region, which is crucial in stabilizing the AF-2 helix in a positive position which permits activation of PPARα (Bénardeau et al., 2009; Bernardes et al., 2013; Li et al., 2018). However, no hydrogen interactions between SCCPs and the AF-2 region were observed or predicted during the present study. These results indicated that SCCPs interacted with the PPARα via an alternative mechanism of binding, which was different from the action of standard PPARα agonists.

Due to the lack of hydrogen bonds with residues on the AF-2 region, SCCPs might have only partial efficacy at the receptor, although SCCPs possess strong binding affinities to PPARα protein. It has been reported that exposure to 1 mg/kg bm/d of PFOA for 21 d significantly upregulated expressions of mRNAs for *Pex11a*, *Eci1*, *Ech1*, *Ehhadh*, and *Acaa1*, which are under control of PPARα signaling in rat liver (Guruge et al., 2006). Based on predictions of molecular docking analyses in the present study, binding affinities of SCCPs with chlorine contents of more than 50% to PPARα were greater than that of PFOA. However, C_{10-13}-CPs (56.5% Cl) only significantly increased expressions of genes downstream of PPARα in livers of male rats, after exposure to the greatest dose of 100 mg/kg bm/d. There were no significant inductions of genes regulated by PPARα in the 1 or 10 mg/kg bm/d of C_{10-13}-CPs (56.5% Cl) exposure groups. These results, together with those of the previous study, indicated that C_{10-13}-CPs (56.5% Cl) have lesser potency as PPARα agonists than does PFOA.

Fig. 4. Effects of exposure to SCCPs on metabolism of fatty acids in rat liver. FA: fatty acid; AC: acylcarnitine; SC: short-chain; MC: medium-chain; LC: long-chain; VLC: very long-chain; Significant differences were indicated in comparison with the control by the *t*-test. *$P < 0.05$; **$P < 0.01$. $N = 8$.

molecular initiating event of ligands binding to the PPARα receptor (Fig. 2). Among these genes, *Pex11a* regulates peroxisome biogenesis; *Decr2*, *Ech1*, *Ehhadh*, and *Acaa1* regulate peroxisomal β-oxidation; *Acadl*, *Acadvl*, *Decr1*, *Eci1*, and *Hadha* regulate mitochondrial β-oxidation; and *Cyp4a1* regulates microsomal ω-oxidation. Up-regulated expressions of mRNA for these genes suggested acceleration of fatty acid oxidation in liver of rat. In liver of the rat, all these genes are tightly regulated by PPARα (Rakhshandehroo et al., 2010). These results suggested activation of the PPARα-mediated signaling pathway by SCCPs. It was hypothesized that various biological responses observed in rodents after exposure to SCCPs, such as peroxisome proliferation

4.3. Exposure to SCCPs disrupted metabolism of fatty acid via PPARα signaling

SCCPs disrupted metabolism of fatty acids via interacting with PPARα. In liver, PPARα is the critical regulator of transport and oxidation of fatty acids (Kersten, 2014). In the present study, effects of exposure to SCCPs on metabolism of fatty acids in rat liver were elucidated by use of pseudo-targeted metabolomics. MELI$_{FA}$ was used to assess overall disruption of fatty acids metabolism by SCCPs. The MELI$_{FA}$ value converts information-rich metabolomics data into an integrated and quantitative endpoint and has been successfully applied in toxicological evaluations (Ren et al., 2018; Wang et al., 2018). Exposure to SCCPs resulted in significantly greater values of the MELI$_{FA}$ in rat liver, which indicated significant perturbation to metabolism of fatty acids by SCCPs.

Results of the metabolomics study confirmed that alterations in expressions of genes coding for enzymes under control of PPARα could result in disorders of metabolism of fatty acids. In rat liver, exposure to all doses of SCCPs resulted in significantly less total contents of quantified fatty acids (Fig. 4), which indicated up-regulation of catabolism of fatty acids. Before being transported into mitochondria where oxidation occurs, LC-FA is first transformed to LC-AC, which serves as an essential intermediate of fatty acid catabolism (Zammit, 1999). Clofibrate, a typical peroxisome proliferator which activates PPARα, resulted in greater concentrations of LC-AC in rat liver (Pande and Parvin, 1980). Modulations of concentrations of LC-AC in rat liver, by exposure to SCCPs, also supported that SCCPs are activators of rat PPARα. Overall, metabolomics data presented here were consistent with the profession of differential expressions of genes, which demonstrated changes in expressions of genes that were caused by interactions between SCCPs and PPARα were mainly responsible for disruption of metabolism of fatty acids in rat liver. The accelerated fatty acid oxidation also suggested an increase in the free radical oxidation of fatty acids in the liver cells, which might be associated with the development of oxidative stress after the influence of SCCPs exposure. In one of our previous studies, we found that exposure for 48 h to SCCPs altered the intracellular redox status in HepG2 cells, in which the stimulated β-oxidation of fatty acids was also observed (Geng et al., 2015).

The genes of L-carnitine transporter and enzymes involved in L-carnitine biosynthesis are also targeted by PPARα (Wen et al., 2010, 2011, 2012). However, no significant inductions of L-carnitine concentrations were observed after SCCPs exposure. It could contribute from the unconventional binding mode between SCCPs and PPARα LBP, which includes only hydrophobic interactions. As mentioned above, SCCPs should have partial efficacy at the PPARα receptor due to the lack of hydrogen bonds with residues on the AF-2 region of PPARα. Thus, SCCPs might not be sufficiently potent to activate genes regulating L-carnitine uptake and biosynthesis. Further detailed analysis is required to confirm this hypothesis in the future.

4.4. Environmental relevance and potential risks to humans

SCCPs pose a potential risk to human health for their ubiquitous occurrences in environmental matrices and human tissues. Results of recent studies have shown that SCCPs are frequently detected in ambient air (Li et al., 2012), sea water (Ma et al., 2014), and soil (Xu et al., 2016) and have also been found in indoor dust, food, drinking water (Gao et al., 2018), and milk (Xia et al., 2017). The range of concentrations of SCCPs in human blood was 14–3500 ng/g and the median value was 98 ng/g (Li et al., 2017). Concentrations of SCCPs in human blood were found to be 10–1000-fold greater than concentrations of PFOA (0.795–30.9 ng/ml) and PFOS (0.925–26.35 ng/ml) (Yeung et al., 2006). According to results of the molecular docking analysis presented here (Supplementary Table S2), PPARα binding affinities of SCCPs with chlorine contents of more than 50% are greater than those of PFOA and PFOS. When chlorine contents of SCCPs

continue to increase to 60%, their affinities for PPARα are comparable and even greater than that of pirinixic acid. These data demonstrated that SCCPs should receive additional attention. Meanwhile, according to our unpublished data (Supplementary Table S3), exposure to 100 or 1 mg/kg bm/d of C$_{10-13}$-CPs (56.5% Cl) for 28 days resulted in an average value of 2.4 or 0.68 mg/kg wet mass (wm) of ΣSCCPs in livers of male rats. It is noteworthy that the internal exposures in the present study were comparable to the ΣSCCPs concentrations measured in human.

PPARα plays a vital role in metabolic regulation of lipids (Kersten et al., 2014). In addition, PPARα also improves atherosclerosis and insulin resistance and provides anti-inflammatory protection (Kersten et al., 2000; Zandbergen and Plutzky, 2007). Dysfunctions in signaling initiated by PPARα, caused by chemicals in the environment have been implicated in diseases of humans (Lau et al., 2010). For example, cardiac-specific overexpression of PPARα in people with diabetes resulted in a more severe cardio-myopathic phenotype (Finck and Kelly, 2002; Finck et al., 2003). Results of previous studies have shown that agonists of PPARα could cause proliferation of peroxisomes and, thereby, cause liver tumors in rodents by a mechanism dependent on PPARα activation. However, it is generally recognized that this mode of action for hepatocarcinogenesis is not relevant in humans (Bility et al., 2004), possibly due to the low expression of PPARα (Palmer et al., 1998) as well as differences in responsiveness of PPARα in humans relative to those in the rat (Mukherjee et al., 1994). However, expression of PPARα can vary by a factor of 10 among individuals (Palmer et al., 1998). For example, PPARα levels comparable to those of mice were observed in one of six humans (Walgren et al., 2000). This finding suggested that some people could be more susceptible to effects of exposure to SCCPs. Overall, although species differences between rat and human exist, the results of our study are still crucial to better understand the adverse effects of SCCPs at the human internal exposure level. The results reported for the first time here should stimulate further investigations regarding the toxicity of SCCPs, in particular, the relevance between SCCPs exposure and metabolic diseases in susceptible populations.

Funding

Conflict of interest

The authors have no real or perceived competing financial interests to declare.

Appendix A. Supplementary data

Supplementary data to this article can be found online at https://doi.org/10.1016/j.ecoenv.2019.06.003.

References

Ali, T.E.S., Legler, J., 2010. Overview of the mammalian and environmental toxicity of chlorinated paraffins. In: Boer, J. (Ed.), Chlorinated Paraffins. Springer Berlin Heidelberg, Berlin, Heidelberg, pp. 135–154.

Bénardeau, A., Benz, J., Binggeli, A., Blum, D., Boehringer, M., Grether, U., Hilpert, H., Kuhn, B., Märki, H.P., Meyer, M., Püntener, K., Raab, S., Ruf, A., Schlatter, D., Mohr, P., 2009. Aleglitazar, a new, potent, and balanced dual PPARα/γ agonist for the treatment of type II diabetes. Bioorg. Med. Chem. Lett 19, 2468–2473.

Bernardes, A., Souza, P.C.T., Muniz, J.R.C., Ricci, C.G., Ayers, S.D., Parekh, N.M., Godoy, A.S., Trivella, D.B.B., Reinach, P., Webb, P., Skaf, M.S., Polikarpov, I., 2013. Molecular mechanism of peroxisome proliferator-activated receptor α activation by WY14643: a new mode of ligand recognition and receptor stabilization. J. Mol. Biol. 425, 2878–2893.

Bility, M.T., Thompson, J.T., McKee, R.H., David, R.M., Butala, J.H., Vanden Heuvel, J.P., Peters, J.M., 2004. Activation of mouse and human peroxisome proliferator-activated receptors (PPARs) by phthalate monoesters. Toxicol. Sci. 82, 170–182.

Brélivet, Y., Rochel, N., Moras, D., 2012. Structural analysis of nuclear receptors: from isolated domains to integral proteins. Mol. Cell. Endocrinol. 348, 466–473.

Bucher, J.R., Alison, R.H., Montgomery, C.A., Huff, J., Haseman, J.K., Farnell, D., Thompson, R., Prejean, J.D., 1987. Comparative toxicity and carcinogenicity of two chlorinated paraffins in F344/N rats and B6C3F1 mice. Toxicol. Sci. 9, 454–468.

Burýšková, B., Bláha, L., Vršková, D., Šimkova, K., Maršalek, B., 2006. Sublethal toxic effects and induction of gGutathione *S*-transferase by short-chain chlorinated paraffins (SCCPs) and C-12 alkane (dodecane) in *Xenopus laevis* frog embryos. Acta Vet. 75, 115–122.

Chen, S., Kong, H., Lu, X., Li, Y., Yin, P., Zeng, Z., Xu, G., 2013. Pseudotargeted metabolomics method and its application in serum biomarker discovery for hepatocellular carcinoma based on ultra high-performance liquid chromatography/triple quadrupole mass spectrometry. Anal. Chem. 85, 8326–8333.

Cooley, H.M., Fisk, A.T., Wiens, S.C., Tomy, G.T., Evans, R.E., Muir, D.C.G., 2001. Examination of the behavior and liver and thyroid histology of juvenile rainbow trout (*Oncorhynchus mykiss*) exposed to high dietary concentrations of C_{10}-, C_{11}-, C_{12}- and C_{14}-polychlorinated *n*-alkanes. Aquat. Toxicol. 54, 81–99.

Feige, J.N., Gerber, A., Casals-Casas, C., Yang, Q., Winkler, C., Bedu, E., Bueno, M., Gelman, L., Auwerx, J., Gonzalez, F.J., Desvergne, B., 2010. The pollutant diethylhexyl phthalate regulates hepatic energy metabolism via species-specific PPARα-dependent mechanisms. Environ. Health Perspect. 118, 234–241.

Fiedler, H., 2010. Short-chain chlorinated paraffins: production, use and international regulations. In: Boer, J. (Ed.), Chlorinated Paraffins. Springer Berlin Heidelberg, Berlin, Heidelberg, pp. 1–40.

Finck, B.N., Han, X., Courtois, M., Aimond, F., Nerbonne, J.M., Kovacs, A., Gross, R.W., Kelly, D.P., 2003. A critical role for PPARα-mediated lipotoxicity in the pathogenesis of diabetic cardiomyopathy: modulation by dietary fat content. Proc. Natl. Acad. Sci. Unit. States Am. 100, 1226–1231.

Finck, B.N., Kelly, D.P., 2002. Peroxisome proliferator-activated receptor α (PPARα) signaling in the gene regulatory control of energy metabolism in the normal and diseased heart. J. Mol. Cell. Cardiol. 34, 1249–1257.

Fletcher, T., Galloway, T.S., Melzer, D., Holcroft, P., Cipelli, R., Pilling, L.C., Mondal, D., Luster, M., Harries, L.W., 2013. Associations between PFOA, PFOS and changes in the expression of genes involved in cholesterol metabolism in humans. Environ. Int. 57–58, 2–10.

Gao, W., Cao, D., Wang, Y., Wu, J., Wang, Y., Wang, Y., Jiang, G., 2018. External exposure to short- and medium-chain chlorinated paraffins for the general population in Beijing, China. Environ. Sci. Technol. 52, 32–39.

Geng, N., Zhang, H., Zhang, B., Wu, P., Wang, F., Yu, Z., Chen, J., 2015. Effects of short-chain chlorinated paraffins exposure on the viability and metabolism of human hepatoma HepG2 cells. Environ. Sci. Technol. 49, 3076–3083.

Glüge, J., Wang, Z., Bogdal, C., Scheringer, M., Hungerbühler, K., 2016. Global production, use, and emission volumes of short-chain chlorinated paraffins – a minimum scenario. Sci. Total Environ. 573, 1132–1146.

Gong, Y., Zhang, H., Geng, N., Xing, L., Fan, J., Luo, Y., Song, X., Ren, X., Wang, F., Chen, J., 2018. Short-chain chlorinated paraffins (SCCPs) induced thyroid disruption by enhancement of hepatic thyroid hormone influx and degradation in male Sprague Dawley rats. Sci. Total Environ. 625, 657–666.

Guruge, K.S., Yeung, L.W.Y., Yamanaka, N., Miyazaki, S., Lam, P.K.S., Giesy, J.P., Jones, P.D., Yamashita, N., 2006. Gene expression profiles in rat liver treated with perfluorooctanoic acid (PFOA). Toxicol. Sci. 89, 93–107.

Harley, K.G., Schall, R.A., Chevrier, J., Tyler, K., Aguirre, H., Bradman, A., Holland, N.T., Lustig, R.H., Calafat, A.M., Eskenazi, B., 2013. Prenatal and postnatal bisphenol A exposure and body mass index in childhood in the CHAMACOS cohort. Environ. Health Perspect. 121, 514–520.

Ishibashi, H., Hirano, M., Kim, E.Y., Iwata, H., 2019. In vitro and in silico evaluations of binding affinities of perfluoroalkyl substances to Baicai seal and human peroxisome proliferator-activated receptor α. Environ. Sci. Technol. 53, 2181–2188.

Kato, Y., Kenne, K., 1996. Inhibition of cell-cell communication by commercial chlorinated paraffins in rat liver epithelial IAR 20 cells. Pharmacol. Toxicol. 79, 23–28.

Kersten, S., 2014. Integrated physiology and systems biology of PPARα. Mol. Metab. 3, 354–371.

Kersten, S., Desvergne, B., Wahli, W., 2000. Roles of PPARs in health and disease. Nature 405, 421.

Lau, C., Abbott, B.D., Corton, J.C., Cunningham, M.L., 2010. PPARs and xenobiotic-induced adverse effects: relevance to human health. PPAR Res. 2010, 954639.

Lejonklou, M.H., Dunder, L., Bladin, E., Pettersson, V., Rönn, M., Lind, L., Waldén, T.B., Lind, P.M., 2017. Effects of low-dose developmental bisphenol A exposure on metabolic parameters and gene expression in male and female Fischer 344 rat offspring. Environ. Health Perspect. 125, 067018.

Li, C.H., Ren, X.M., Ruan, T., Cao, L.Y., Xin, Y., Guo, L.H., Jiang, G.B., 2018. Chlorinated polyfluorinated ether sulfonates exhibit higher activity toward peroxisome proliferator-activated receptors signaling pathways than perfluorooctanesulfonate. Environ. Sci. Technol. 52, 3232–3239.

Li, H., Fu, J., Zhang, A., Zhang, Q., Wang, Y., 2016. Occurrence, bioaccumulation and long-range transport of short-chain chlorinated paraffins on the Fildes Peninsula at King George Island, Antarctica. Environ. Int. 94, 408–414.

Li, Q., Li, J., Wang, Y., Xu, Y., Pan, X., Zhang, G., Luo, C., Kobara, Y., Nam, J.J., Jones,

K.C., 2012. Atmospheric short-chain chlorinated paraffins in China, Japan, and South Korea. Environ. Sci. Technol. 46, 11948–11954.

Li, T., Wan, Y., Gao, S., Wang, B., Hu, J., 2017. High-throughput determination and characterization of short-, medium-, and long-chain chlorinated paraffins in human blood. Environ. Sci. Technol. 51, 3346–3354.

Liu, L., Li, Y., Coelhan, M., Chan, H.M., Ma, W., Liu, L., 2016. Relative developmental toxicity of short-chain chlorinated paraffins in Zebrafish (*Danio rerio*) embryos. Environ. Pollut. 219, 1122–1130.

Livak, K.J., Schmittgen, T.D., 2001. Analysis of relative gene expression data using real-time quantitative PCR and the $2^{-\Delta\Delta CT}$ method. Methods 25, 402–408.

Ma, X., Zhang, H., Wang, Z., Yao, Z., Chen, J., Chen, J., 2014. Bioaccumulation and trophic transfer of short chain chlorinated paraffins in a marine food web from Liaodong Bay, North China. Environ. Sci. Technol. 48, 5964–5971.

Mandard, S., Müller, M., Kersten, S., 2004. Peroxisome proliferator-activated receptor α target genes. Cell. Mol. Life Sci. 61, 393–416.

Matilla-Santander, N., Valvi, D., Lopez-Espinosa, M.J., Manzano-Salgado, C.B., Ballester, F., Ibarluzea, J., Santa-Marina, L., Schettgen, T., Guxens, M., Sunyer, J., Vrijheid, M., 2017. Exposure to perfluoroalkyl substances and metabolic outcomes in pregnant women: evidence from the Spanish INMA birth cohorts. Environ. Health Perspect. 125, 117004.

Mukherjee, R., Jow, L., Noonan, D., McDonnell, D.P., 1994. Human and rat peroxisome proliferator activated receptors (PPARs) demonstrate similar tissue distribution but different responsiveness to PPAR activators. J. Steroid Biochem. Mol. Biol. 51, 157–166.

Nilsen, O.G., Toftgard, R., Glaumann, H., 1981. Effects of chlorinated paraffins on rat liver microsomal activities and morphology. Importance of the length and the degree of chlorination of the carbon chain. Arch. Toxicol. 49, 1–13.

Palmer, C.N.A., Hsu, M.H., Griffin, K.J., Raucy, J.L., Johnson, E.F., 1998. Peroxisome proliferator activated receptor-α expression in human liver. Mol. Pharmacol. 53, 14–22.

Pande, S.V., Parvin, R., 1980. Clofibrate enhancement of mitochondrial carnitine transport system of rat liver and augmentation of liver carnitine and γ-butyrobetaine hydroxylase activity by thyroxine. Biochim. Biophys. Acta 617, 363–370.

Poulsen, L.l.C., Siersbæk, M., Mandrup, S., 2012. PPARs: fatty acid sensors controlling metabolism. Semin. Cell Dev. Biol. 23, 631–639.

Rakhshandehroo, M., Knoch, B., Müller, M., Kersten, S., 2010. Peroxisome proliferator-activated receptor alpha target genes. PPAR Res. 2010 20.

Ren, X., Zhang, H., Geng, N., Xing, L., Zhao, Y., Wang, F., Chen, J., 2018. Developmental and metabolic responses of zebrafish (*Danio rerio*) embryos and larvae to short-chain chlorinated paraffins (SCCPs) exposure. Sci. Total Environ. 622–623, 214–221.

Riedl, J., Schreiber, R., Otto, M., Heilmeier, H., Altenburger, R., Schmitt-Jansen, M., 2015. Metabolic effect level index links multivariate metabolic fingerprints to ecotoxicological effect assessment. Environ. Sci. Technol. 49, 8096–8104.

Serrone, D.M., Birtley, R.D.N., Weigand, W., Millischer, R., 1987. Toxicology of chlorinated paraffins. Food Chem. Toxicol. 25, 553–562.

Tomy, G.T., Billeck, B., Stern, G.A., 2000. Synthesis, isolation and purification of C_{10}–C_{13} polychloro-*n*-alkanes for use as standards in environmental analysis. Chemosphere 40, 679–683.

Uemura, H., Arisawa, K., Hiyoshi, M., Kitayama, A., Takami, H., Sawachika, F., Dakeshita, S., Nii, K., Satoh, H., Sumiyoshi, Y., Morinaga, K., Kodama, K., Suzuki, T.-i., Nagai, M., Suzuki, T., 2009. Prevalence of metabolic syndrome associated with body burden levels of dioxin and related compounds among Japan's general population. Environ. Health Perspect. 117, 568–573.

United Nations Environment Program (UNEP), 2017. The New POPs under the Stockholm Convention. http://www.pops.int/TheConvention/ThePOPs/TheNewPOPs/tabid/2511, Accessed date: 31 July 2018.

Walgren, J.E., Kurtz, D.T., McMillan, J.M., 2000. Expression of PPAR(alpha) in human hepatocytes and activation by trichloroacetate and dichloroacetate. Res. Commun. Mol. Pathol. Pharmacol. 108, 116–132.

Wang, F., Zhang, H., Geng, N., Ren, X., Zhang, B., Gong, Y., Chen, J., 2018. A metabolomics strategy to assess the combined toxicity of polycyclic aromatic hydrocarbons (PAHs) and short chain chlorinated paraffins (SCCPs). Environ. Pollut. 234, 572–580.

Wang, F., Zhang, H., Geng, N., Zhang, B., Ren, X., Chen, J., 2016. New insights into the cytotoxic mechanism of hexabromocyclododecane from a metabolomic approach. Environ. Sci. Technol. 50, 3145–3153.

Warnasuriya, G.D., Elcombe, B.M., Foster, J.R., Elcombe, C.R., 2010. A mechanism for the induction of renal tumours in male Fischer 344 rats by short-chain chlorinated paraffins. Arch. Toxicol. 84, 233–243.

Wen, G., Ringseis, R., Eder, K., 2010. Mouse OCTN2 is directly regulated by peroxisome proliferator-activated receptor α (PPARα) via a PPRE located in the first intron. Biochem. Pharmacol. 79, 768–776.

Wen, G., Kühne, H., Rauer, C., Ringseis, R., Eder, K., 2011. Mouse γ-butyrobetaine dioxygenase is regulated by peroxisome proliferator-activated receptor α through a PPRE located in the proximal promoter. Biochem. Pharmacol. 82, 175–183.

Wen, G., Ringseis, R., Rauer, C., Eder, K., 2012. The mouse gene encoding the carnitine biosynthetic enzyme 4-N-trimethylaminobutyraldehyde dehydrogenase is regulated by peroxisome proliferator-activated receptor α. Biochim. Biophys. Acta, Gene Regul. Mech. 1819, 357–365.

Xia, D., Gao, L., Zheng, M., Li, J., Zhang, L., Wu, Y., Tian, Q., Huang, H., Qiao, L., 2017. Human exposure to short- and medium-chain chlorinated paraffins via mothers' milk in Chinese urban population. Environ. Sci. Technol. 51, 608–615.

Xu, J., Gao, Y., Zhang, H., Zhan, F., Chen, J., 2016. Dispersion of short- and medium-chain chlorinated paraffins (CPs) from a CP production plant to the surrounding surface soils and coniferous leaves. Environ. Sci. Technol. 50, 12759–12766.

Yeung, L.W.Y., So, M.K., Jiang, G., Taniyasu, S., Yamashita, N., Song, M., Wu, Y., Li, J., Giesy, J.P., Guruge, K.S., Lam, P.K.S., 2006. Perfluorooctanesulfonate and related

fluorochemicals in human blood samples from China. Environ. Sci. Technol. 40, 715–720.

Zammit, V.A., 1999. Carnitine acyltransferases: functional significance of subcellular distribution and membrane topology. Prog. Lipid Res. 38, 199–224.

Zandbergen, F., Plutzky, J., 2007. PPARα in atherosclerosis and inflammation. Biochim. Biophys. Acta 1771, 972–982.

Zeng, L., Lam, J.C.W., Chen, H., Du, B., Leung, K.M.Y., Lam, P.K.S., 2017. Tracking dietary sources of short- and medium-chain chlorinated paraffins in marine mammals

through a subtropical marine food web. Environ. Sci. Technol. 51, 9543–9552.

Zhang, Q., Wang, J., Zhu, J., Liu, J., Zhang, J., Zhao, M., 2016. Assessment of the endocrine-disrupting effects of short-chain chlorinated paraffins in *in vitro* models. Environ. Int. 94, 43–50.

Zhao, H., Caflisch, A., 2014. Discovery of dual ZAP70 and Syk kinases inhibitors by docking into a rare C-helix-out conformation of Syk. Bioorg. Med. Chem. Lett 24, 1523–1527.

1   *Supplementary material for*

2   **Short-chain chlorinated paraffins (SCCPs) disrupt hepatic fatty**

3   **acid metabolism in liver of male rat via interacting with**

4   **peroxisome proliferator-activated receptor α (PPARα)**

5

6   Yufeng Gong[a], Haijun Zhang[a,*], Ningbo Geng[a], Xiaoqian Ren[a,b], John P.

7   Giesy[c,d], Yun Luo[a,b], Liguo Xing[e], Ping Wu[a], Zhengkun Yu[a], Jiping Chen[a]

8

9   [a]*CAS Key Laboratory of Separation Sciences for Analytical Chemistry, Dalian*

10   *Institute of Chemical Physics, Chinese Academy of Sciences, Dalian 116023, Liaoning,*

11   *China*

12   [b]*University of Chinese Academy of Sciences, Beijing 100049, China*

13   [c]*Department of Veterinary Biomedical Sciences and Toxicology Centre, University of*

14   *Saskatchewan, Saskatoon SK S7N 5B4, Saskatchewan, Canada*

15   [d]*Department of Environmental Science, Baylor University, Waco TX 76706, Texas,*

16   *United States*

17   [e]*Safety Evaluation Center of Shenyang Research Institute of Chemical Industry Ltd,*

18   *Shenyang 110021, Liaoning, China*

19

20   *Number of pages: 16*

21   *Number of figures: 5*

22   *Number of tables: 3*

Contents:

1. Primer sequences for the genes tested

Table S1. Primer sequences used for rat liver.

Gene symbol	Description	Accession number	Primer sequence (5'-3')[1]
Pex11a	Peroxisomal biogenesis factor 11 alpha	NM_053487	F: GGCAAAGAGGCGGTGGTAAC R: GCGGTTCAGGTTGGCTAATG
Decr2	Peroxisomal 2,4-dienoyl-CoA reductase	NM_171996	F: GCATCCTTGCTGAGCACTACC R: GCTGCCTCTGTTGAGTCCGT
Ech1	Enoyl-CoA hydratase 1, peroxisomal	NM_022594	F: CAAGAGTCCTGTGGCTGTGC R: CTGACTTGATGATGTCCTGGGT
Ehhadh	Enoyl-CoA hydratase/3-hydroxyacyl CoA dehydrogenase	NM_133606	F: TTGGAGTTCCTGTTGCTCTTGA R: GCGGGGTTCTATGGGTTTATC
Acaa1	Acetyl-CoA acyltransferase 1A	NM_012489	F: AATGTGGCTGAGCGGTTTG R: GAGACACGGTGATGGTTTTCC
Acadl	Acyl-CoA dehydrogenase, long chain	NM_012819	F: GGGCTGGAAGTGACTTACAAGG R: TGGTGACGGCCACTACGAT
Acadvl	Acyl-CoA dehydrogenase, very long chain	NM_012891	F: AAGGAACCAGGGGTAGAGCG R: CATGCAGCCTTGTAGAGCCAC
Decr1	2,4-dienoyl-CoA reductase 1	NM_057197	F: CTCAGTTCTGCTGCAAACATGG R: CTTTGATACAGGGTTTTCGTTCC
Eci1	Enoyl-CoA delta isomerase 1	NM_017306	F: GGCTGAGGCTCTACTTGTCCA R: GTCCGCCATTATCCTGTAGTCA

Hadha	hydroxyacyl-CoA dehydrogenase trifunctional multienzyme complex subunit alpha	NM_130826	F: CTACTCCGCGACCTTGCTAAC
			R: TCGGTCTTTCTCCTGCTTCC
Cyp4a1	Cytochrome P450, family 4, subfamily a, polypeptide 1	NM_175837	F: TCCCAAGTGCCTTTCCTCG
			R: GTTGTCCATTCAGCAAGAGCA
Actb	Actb, beta	NM_031144	F: TGCTGACAGGATGCAGAAGG
			R: TGGAAGGTGGACAGTGAGGC
Gapdh	Glyceraldehyde-3-phosphate dehydrogenase	NM_017008	F: GTATCGGACGCCTGGTTAC
			R: CTTGCCGTGGGTAGAGTCAT

Note: Specific primers were designed based on sequence data from the GenBank (https://www.ncbi.nlm.nih.gov/genbank/).

1 **2. Dataset and the binding affinities predicted by LeDock**

2 **Table S2.** Predicted binding affinity (kcal/mol) on human PPARα.

Compound	CAS No.	Chlorine contents	PPARα binding affinity
C_{10}-Cl_1	1002-69-3	20.08%	-5.30
C_{10}-Cl_2	2162-98-3	33.60%	-5.82
C_{10}-Cl_3	--	43.33%	-6.51
C_{10}-Cl_4	205646-11-3	50.66%	-6.75
C_{10}-Cl_5	1637297-61-0	56.39%	-7.14
C_{10}-Cl_6	--	60.98%	-7.54
C_{10}-Cl_7	890302-88-2	64.75%	-8.36
C_{10}-Cl_8	--	67.90%	-8.40
C_{10}-Cl_9	--	70.56%	-8.74
C_{10}-Cl_{10}	--	72.85%	-9.16
C_{11}-Cl_1	2473-03-2	18.60%	-5.33
C_{11}-Cl_2	822-07-1	31.51%	-5.93
C_{11}-Cl_3	--	40.99%	-6.55
C_{11}-Cl_4	210049-49-3	48.25%	-7.05
C_{11}-Cl_5	--	53.98%	-7.71
C_{11}-Cl_6	1428966-54-4	58.63%	-8.14
C_{11}-Cl_7	--	62.47%	-8.33
C_{11}-Cl_8	--	65.69%	-8.53
C_{11}-Cl_9	--	68.44%	-8.48
C_{11}-Cl_{10}	--	70.81%	-8.69
C_{11}-Cl_{11}	--	72.88%	-9.97
C_{12}-Cl_1	112-52-7	17.33%	-5.87
C_{12}-Cl_2	3922-28-9	29.66%	-6.24
C_{12}-Cl_3	--	38.89%	-6.93
C_{12}-Cl_4	210115-98-3	46.05%	-7.31
C_{12}-Cl_5	--	51.77%	-8.06
C_{12}-Cl_6	1428966-55-5	56.45%	-8.70
C_{12}-Cl_7	1005111-47-6	60.34%	-8.69
C_{12}-Cl_8	--	63.63%	-9.38
C_{12}-Cl_9	--	66.45%	-9.18
C_{12}-Cl_{10}	--	68.89%	-9.14
C_{12}-Cl_{11}	--	71.02%	-9.63

$C_{12}-Cl_{12}$	--	72.90%	-9.31
$C_{13}-Cl_1$	822-13-9	16.22%	-5.90
$C_{13}-Cl_2$	822-14-0	28.02%	-6.68
$C_{13}-Cl_3$	--	36.99%	-7.31
$C_{13}-Cl_4$	--	44.05%	-7.65
$C_{13}-Cl_5$	--	49.74%	-8.16
$C_{13}-Cl_6$	1428966-56-6	54.42%	-8.63
$C_{13}-Cl_7$	--	58.35%	-9.23
$C_{13}-Cl_8$	--	61.69%	-9.59
$C_{13}-Cl_9$	--	64.56%	-8.59
$C_{13}-Cl_{10}$	--	67.06%	-9.31
$C_{13}-Cl_{11}$	--	69.25%	-9.46
$C_{13}-Cl_{12}$	--	71.19%	-9.7
$C_{13}-Cl_{13}$	--	72.92%	-10.1
Pirinixic acid	50892-23-4	--	-8.49
PFOA	45285-51-6	--	-6.30
PFOS	45298-90-6	--	-7.37
n-decane acid	334-48-5	--	-5.24
n-undecanoic acid	112-37-8	--	-5.60
n-dodecanoic acid	143-07-7	--	-5.92
n-tridecanoic acid	638-53-9	--	-6.29

3   Note: Molecular docking was performed by Ledock program (http://lephar.com).

4

3. Details on sample preparation and instrumental analysis

Sample preparation

Sample was mixed with 1 mL of ultrapure water, homogenized, and then ultra-sonicated for 5 min in an ice-water bath. The sample were subsequently freeze-dried and extracted with a mixture of methanol/water (4: 1, v: v). Soon afterwards, the solution was vortexed for 30 min, and then centrifuged for 20 min at 13,000 × g and 8 °C. Finally, the supernatant was filtered by an organic phase filter and transferred to a vial for metabolite analysis. Prior to extraction, three kinds of internal standards (i.e., octanoyl (8, 8, 8-D3)-L-carnitine, hendecanoic acid, and nonadecanoic acid) were spiked into the sample for the quality control of sample preparation and instrumental analysis.

UHPLC/Q-TOF MS for Untargeted Tandem MS

For untargeted tandem MS, the "auto MS/MS" function of the Q-TOF MS system with data-dependent acquisition was performed in positive ion mode and negative ion mode, respectively. For positive ion mode, 5 μL of extract containing metabolites was injected into the UHPLC/Q-TOF MS system with an ACQUITY UPLC BEH C8 column (2.1 mm × 100 mm × 1.7 μm, Waters, USA) maintained at 50 °C. Water and acetonitrile both containing 0.1% (v/v) formic acid were used as mobile phases A and B, respectively. The flow rate was 0.35 mL/min, and the gradient elution was as follows (time, %B): 0 min, 10%; 3 min, 40%; 15 min, 100%, and maintained for 5 min; 20.1 min, 10%, and re-equilibrated for 2.9 min. The mass spectrometer was operated with a capillary voltage of 4000 V, fragmentor voltage of 175 V, skimmer voltage of 65 V, nebulizer gas (N_2) pressure at 45 psi, drying gas (N_2) flow rate of 9 L/min, and a temperature of 350 °C. Five most intense precursors were

30 chosen within one full scan cycle (0.25 s) with a precursor ion scan range of m/z

31 100−1000 and a tandem mass scan range of m/z 40−1000. The collision energies were

32 set at 10, 20, 30, and 40 eV, and all samples were analyzed to obtain abundant and

33 complementary product ion information.

34   For negative ion mode, 5 μL of extract containing metabolites was injected into

35 the UHPLC/Q-TOF MS system with an ACQUITY UPLC HSS T3 column (2.1 mm ×

36 100 mm × 1.8 μm, Waters, USA) maintained at 50 °C. Water and methanol both

37 containing 5 mmol/L ammonium bicarbonate were used as mobile phases A and B,

38 respectively. The flow rate was also 0.35 mL/min, and the gradient elution was as

39 follows (time, %B): 0 min, 2%; 3 min, 42%; 12 min, 100%, and maintained for 4 min;

40 16.1 min, 2%, and re-equilibrated for 3.9 min. The mass spectrometer was operated

41 with a capillary voltage of 3500 V, fragmentor voltage of 175 V, skimmer voltage of

42 65 V, nebulizer gas (N_2) pressure at 45 psi, drying gas (N_2) flow rate of 9 L/min, and a

43 temperature of 350 °C. Five most intense precursors were chosen within one full scan

44 cycle (0.25 s) with a precursor ion scan range of m/z 100−1000 and a tandem mass

45 scan range of m/z 40−1000. The collision energies were set at −10, −20, −30, and −40

46 eV, and all samples were analyzed to obtain abundant and complementary product ion

47 information.

48   After data acquisition, the "Find by Auto MS/MS" function of MassHunter

49 Qualitative Analysis software was used to automatically extract ion pair information

50 for subsequent MRM detection. The retention time window was set to 0.15 min; the

51 MS/MS threshold was set to 100, and the mass match tolerance was set to 0.02 Da.

52 The single mass expansion was set to symmetric 100 ppm, and the persistent

53 background ions, such as reference mass ions, were excluded. After execution,

54 detected ion pairs with information about the precursor ion, product ions, retention

time, and collision energy were exported to a spreadsheet. Ion pairs were selected on the basis of the following rules: different precursor ions eluted in the neighboring time range were scrutinized to exclude the isotopic, fragmentation, adduct, and dimer ions; and the product ion that appeared with the most applied collision energy and with the highest intensity was selected as the characteristic product ion.

UHPLC/Q-Trap MRM MS for Pseudo-targeted Metabolomic Analysis

A Waters Acquity Ultra Prerformance liquid chromatography system (UHPLC) coupled online to an ABI Q-Trap 5500 (AB SCIEX, USA) via an electrospray ionization (ESI) interface was adopted for pseudo-targeted metabolomics analysis using the spreadsheet produced from the analysis of UHPLC/Q-TOF MS. The same chromatographic condition, including chromatographic column, mobile phases, and gradient elution procedure, was performed on both UHPLC/Q-TOF MS system and UHPLC/Q-Trap MS system.

For positive ion mode, The MS instrumental parameters were set as those for the following: source temperature, 550 °C; gas I, 40 arbitrary units; gas II, 40 arbitrary units; curtain gas, 35 arbitrary units; ion spray voltage, 5500 V. The internal standard octanoyl (8, 8, 8-D3)-L-carnitine was used for normalizing the peak areas of all other analytes.

For negative ion mode, The MS instrumental parameters were set as follows: source temperature, 550 °C; gas I, 40 arbitrary units; gas II, 40 arbitrary units; curtain gas, 35 arbitrary units; ion spray voltage, −4500 V. Hendecanoic acid and nonadecanoic acid served as internal standards to normalize the peak areas of all other analytes.

80 **4. Calculation of MELI**

81   The metabolic change (MC$_i$) of each metabolite in a sample was calculated

82   (Equation 1).

83 $$MC_i = e^{|\ln(A_i)|} - e^{|\ln(1)|} \tag{1}$$

84   where A$_i$ is the ratio of the relative abundance of a specific metabolite (i) in exposure

85   group to the mean relative abundance of this metabolite in the control group, and ln (1)

86   is used to subtract the metabolic level of the control group. Then, the overall

87   metabolomics alteration of a sample was summarized as the accumulated changes of

88   all n quantified metabolites (Equation 2).

89 $$\text{MELI} = \left(\sum_{i=1}^{i=n} MC_i\right)\Big/ n \tag{2}$$

90

91   **5. Endogenous PPARα expression in 293T cells**
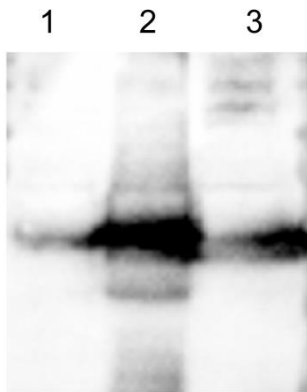
92

93   **Figure S1.** Western blot analysis. Western blot was performed to examine the

94   endogenous PPARα expression in 293T cells according to a routine method. We used

95   a human PPARα polyclonal antibody in this experiment. Lane 1: 293T cells

96   transfected only with empty vector; Lane 2: 293T cells transfected with human

97   PPARα expression vector; Lane 3: MCF-7 cells.

98

99 **6. MTT assays**

100   293T cells (7000 cells/well) were seeded overnight and treated them with various

101 concentrations of C_{10-13}-CPs (56.5% Cl), pirinixic acid or dimethyl sulfoxide (DMSO)

102 (vehicle) alone for 24 hours. Then, we evaluated cell viability using 3-[4,

103 5-dimethylthiazolyl-2]-2, 5-diphenyltetrazoliumbromide (MTT) assay (Sigma, China)

104 according to the manufacturer's directions. The absorbance was read at a wavelength

105 of 492 nm with a multiwall microplate reader (Tecan Infinite F50). The cell viability

106 was calculated by setting the viability of the control cells as 100%.
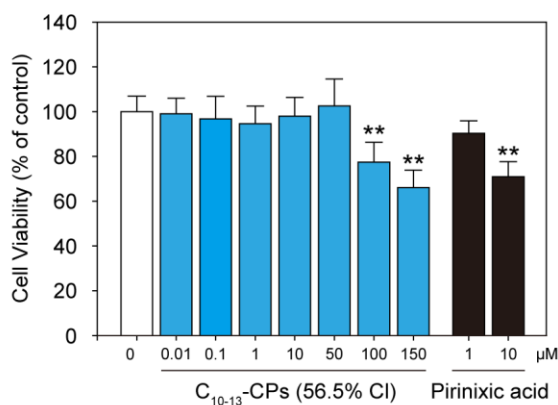
107

108 **Figure S2.** Viability of 293T cells exposed to C_{10-13}-CPs or pirinixic acid at various

109 concentrations for 24 hours. 0.5% DMSO served as the solvent control. Significant

110 differences were indicated in comparison of the control. * $P < 0.05$; ** $P < 0.01$. $N =$

111 6.

112

113 **7. Validity of the dual-luciferase assay**
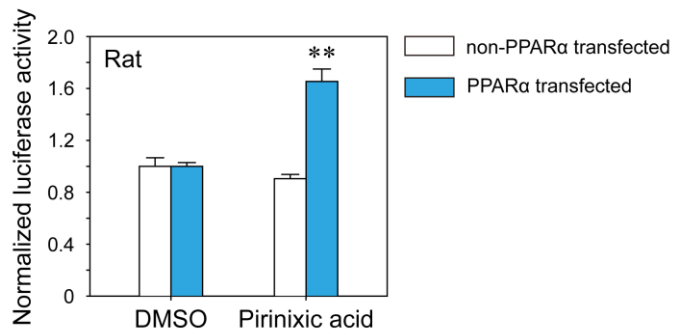
114

115 **Figure S3.** Transcriptional activities of PPARα by pirinixic acid at a concentration of

116 1 μM using *in vitro* luciferase reporter gene assay. Bars indicate the fold induction of

117 transcriptional activities in 293T cells into which PPARα (blue bars) or non-PPARα

118 (white bars) expression vector was transfected. Asterisk denotes statistical difference

119 ($P < 0.05$; $N = 3$) from the transcriptional activities in control cells treated with 0.5%

120 DMSO (vehicle).

121

122   **8. MELI values for fatty acid metabolism**
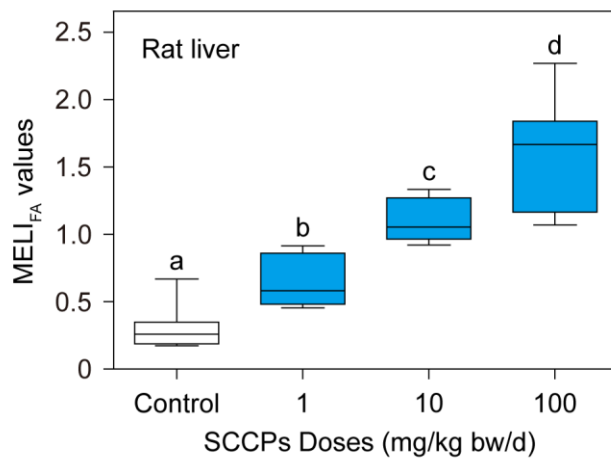
123

124   **Figure S4.** Metabolic effect level index (MELI) values for the fatty acid metabolism

125   in rat liver. Values with different letters denote statistically significant differences

126   according to a one-way ANOVA analysis ($P < 0.01$).

127

9. Binding mode of PFOA in the LBP of human PPARα
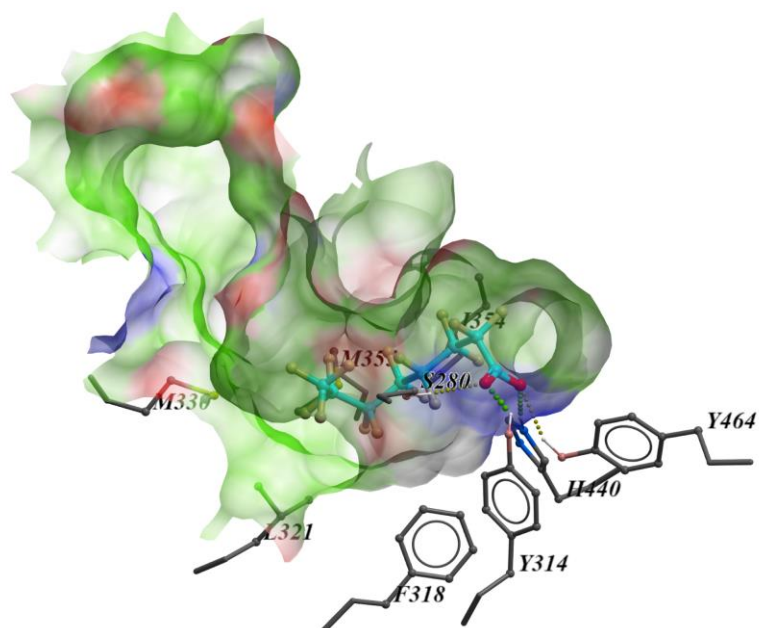
129

130   **Figure S5.** Predicted binding mode of PFOA in the LBP of human PPARα (PDB code

131   2P54). Binding pocket is illustrated by molecular surface with carbon in green, oxygen

132   in red, and nitrogen in blue. Protein residues within 5 Å of the ligand are shown in stick

133   with carbon in grey, oxygen in red, and nitrogen in blue. PFOA was shown with carbon

134   in cyan.

135

10. ∑SCCPs concentrations in male rat liver after SCCPs exposure

Table S3. ∑SCCPs concentrations in male rat liver after exposure to 100 or 1 mg/kg bm/d of C_{10-13}-CPs (56.5% Cl) for 28 days.

Exposure doses (mg/kg bm/d)	Mean ∑SCCPs concentrations (mg/kg wm)
Control	Not detected
1	0.68
100	2.37

Note: ∑SCCPs were measured in male rat liver samples collected after 28 days of oral administration to 0, 1, or 100 mg/kg bm/d of C_{10-13}-CPs (56.5% Cl). Samples were analyzed using a previously published methodology (Gao et al., 2011) involving extraction, cleanup and final determination performed on a trace gas chromatograph coupled to a Trace DSQ II mass spectrometer in ECNI mode (GC/ECNI-MS, Thermo, USA). Approximately 100 mg of the liver samples were extracted with ultrasonic solvent extraction, purified on a multilayer silica gel column, then evaporated and redissolved in 20 μL of the internal standard solution ($^{13}C_6$-α-HCH in *n*-nonane) for the instrumental analysis. Chromatographic separation was performed with a capillary DB-5 column (J&W Scientific, USA). Three samples from each group were subjected to the quantitative analysis, and the concentrations of SCCPs were finally calculated based on the liver weight.

Supplemental Reference:

Gao,Y., Zhang, H.J., Chen, J.P., Zhang, Q., Tian, Y.Z., Qi, P.P., Yu, Z.K., 2011. Optimized cleanup method for the determination of short chain polychlorinated *n*-alkanes in sediments by high resolution gas chromatography/electron capture negative ion–low resolution mass spectrometry. Anal. Chim. Acta. 703, 187–193.